Indian Journal of Chemical Technology
Vol. 23, November, 2016 pp. 453-461

Fischer-Tropsch synthesis over potassium-promoted Co-Fe/SiO_2 catalyst

Mohsen Mansouri[1] & Hossein Atashi*,[2]

[1]Department of Chemical Engineering, University of Ilam, Ilam 69315-516, Iran

[2]Department of Chemical Engineering, University of Sistan and Baluchestan, Zahedan 98164-161, Iran

E-mail: atashi.usb@gmail.com, h.ateshi@hamoon.usb.ac.ir

Received 12 September 2014; accepted 16 October 2015

Experiments for the kinetic of Fischer-Tropsch reaction (hydrocarbon formation) have been carried out over the potassium-promoted Co-Fe/90wt % SiO_2 catalyst in a fixed bed micro-reactor over a range of operating conditions. Reaction rate equations are derived on the basis of the Langmuir-Hinshelwood-Hougen-Watson (LHHW) type models for the FT reactions. Seven kinetic expressions for CO consumption have been proposed and interaction between adsorption CO and dissociated adsorption hydrogen as the controlling step give the most plausible kinetic model. The product distributions in FT synthesis are found to be strongly influenced by temperature and pressure, and optimum hydrocarbon selectivity C_2-C_3 light olefins is obtained at 260°C and 8 bar. The value of activation energy for CO consumption confirms that intraparticle mass transport is not significant.

Keywords: Fischer-Tropsch synthesis, Co-Fe catalyst, Kinetics modeling, Light olefins

One of the used synthesis process in production of C_2-C_3 alkenes, gasoline and diesel is Fischer-Tropsch synthesis (FTS) that have the most promising development option for the environmentally sound production of hydrocarbons and fuels from synthesis gas at elevated pressure and temperature[1,2]. Selective formation of such distribution of products by FTS requires a deep molecular study of the CO hydrogenation reactions over a wide range of catalysts[3]. Iron and cobalt are the most promising FTS catalysts and the combination of Co-Fe catalysts leads to Co-Fe alloy formation which favors the formation of alkenes with or without promoters[4-7]. Interest in the development of more selective and active Co-Fe catalyst and more effective FTS process technologies and reactors increased dramatically in the past decades[2,8]. The FTS process with Co catalysts is not complex due to the irreversible and expensive changes in the catalyst however with Fe catalyst, the physical and chemical nature of the FTS with iron catalyst is significantly improve by the wax and carbon deposition due to formation of carbides and magnetite[9]. The FTS preferred catalysts for hydrocarbon production is cobalt-based catalysts due to their low activity and selectivity for the water gas shift reaction and high activity and selectivity for long chain paraffins[10]. The past researches on the FTS catalysts in the patent literature indicate that the Fe catalyst could influence quite dramatically by the addition of small amounts of Co which enhance the activity of this catalyst in comparison to the other metal oxides and the Co-Fe combination is the most promising catalyst for light olefin production from synthesis gas[3,4]. According to the past researches, a few catalysts are suitable to improve the C_2-C_3 fraction due to the thermodynamic and kinetic limitations of the FTS reactions and some examples such as iron and/or cobalt based catalysts on partially reducible oxide supports such as TiO_2 instead of the conventional supports such as Al_2O_3 are reported in the literature[3]. The general effects of promoters on the iron catalysts behavior have been studied in many researches in the past decade and the most essential promoters in Fe catalysts for the FTS process are the group IA metals such as potassium which have obvious effect on both the activity and the selectivity of Fe catalysts[3].

In recent decade, numerous equations use in FTS study such as many researchers have been attempting to suppose the rate of Fischer-Tropsch reaction by Langmuir-Hougen-Watson (LHHW) or a power law rate equation[11-14]. An overview of the rate expressions developed for Fe catalysts is given by Huff and Satterfield[15] and for Co catalysts have been summarized by Yates and Satterfield[16]. For cobalt catalysts, the first researches show that the CO

consumption is proportional to the rate of desorption of hydrocarbon chains growing on the catalyst surface which these growing chain concentration is empirically associated to the 2nd order of hydrogen partial pressure and 1st order of CO partial pressure[17]. Huff and Satterfield[15] and Rautavuoma and van der Baan[18] declared that the rate of CO consumption can be modeled by assuming the rate of the monomer formation as the rate controlling step for a reduced fused magnetite and a cobalt catalyst in the same way. This assumption indicates that all elementary reactions except the controlling step are close to equilibrium and the developed rate equation describes the experimental results practically well in certain ranges of experimental conditions[17].

Kinetic expressions for CO hydrogenation and product distributions on impregnated silica supported cobalt–iron catalysts are not to be found in the studies giving the activity/selectivity relationships. Mirzaei *et al.*[3] reports the effect of operating conditions such as reaction temperatures and pressures and hydrogen to CO molar ratio in the catalytic performance on the SiO_2 supported Fe-Co catalyst prepared by sol-gel route. In accordance with the purpose of this paper is to investigate of the CO hydrogenation on the SiO_2 supported Fe-Co catalysts prepared by impregnation route promoted by potassium. The kinetic model for CO consumption in the FTS has been established on the basis of the correlation between experimental data and supposed reaction mechanism sets. The proper model was obtained and parameters were calculated. Also, in this work, attempt has been made to extensively report the influence of reaction temperatures and pressures on the products selectivity.

Experimental Section

Catalyst preparation

Using conventional method of impregnation a 60%Co/40%Fe/90wt%SiO_2/1.5wt%K catalyst, which has a high value of olefin/paraffin ratio and the chain growth probability, was prepared as discussed in this section. The catalysts were prepared by incipient impregnation of SiO_2 with aqueous cobalt nitrate ($Co(NO_3)_2.6H_2O$) (0.5 M) (99%, Merck) and iron nitrate ($Fe(NO_3)_2.6H_2O$) (0.5 M) (99%, Merck) and potassium nitrate (KNO_3) (0.5 M) (99%, Merck) solutions. The SiO_2 support was first calcined at 600°C in flowing air for 6 h before impregnation. For 60%Co/40%Fe/90wt%SiO_2/1.5wt%K catalyst, the solution of proper amount of cobalt, iron and potassium nitrate was prepared and was directly dispersed through a spray needle onto the support. The impregnated support was then dried at 120°C for 16 h. In order to obtain the final catalyst, the precursor was then calcined at 550°C for 6 h.

Characterization techniques

The BET surface area (BET) was measured using a N_2 adsorption-desorption isotherm at liquid nitrogen temperature (-196°C), using a NOVA 2000 instrument (Quantachrome, USA). Prior to the adsorption–desorption measurements, all of the samples comprising precursors and calcined catalysts were degassed at 200°C in a N_2 flow for 3 h to remove the moisture and other adsorbates.

The morphology of catalysts and their precursors was observed by means of an S-360 Oxford Eng scanning electron microscopy (USA).

Catalyst testing

FTS was carried out in a fixed-bed micro-reactor made of stainless steel with an inner diameter of 20 mm. All gas lines to the reactor bed were made from 1/4″ stainless steel tubing. Three mass flow controllers (Brooks, Model, 5850E) were used to adjust automatically flow rate of the inlet gases comprising CO, H_2 and N_2 (purity of 99.99%). Mixture of CO, H_2 and N_2 were subsequently introduced into the reactor, which was placed inside a tubular furnace (Atbin, Model ATU 150-15). Prior to the reaction the catalysts were reduced in situ using H_2 (30 ml/min) and N_2 (30 ml/min) mixture gas at 350°C for 16 h. In each test, 1.0 g catalyst was loaded and the reactor operated about 12 h to ensure attaining the steady state operating conditions.

The catalyst was extremely fine particles so intraparticle diffusion could be neglected. The gas hourly space velocity (GHSV) increased to the value in which the CO conversion was almost the same for a variety of catalyst weight which indicates that external diffusion can be neglected above this GHSV. Hence, the kinetic experiments were conducted free from internal and external mass transfer limitations.

To minimize temperature and concentration gradients, all steady state kinetic experimental data were collected in the differential fixed-bed micro-reactor with a maximum conversion below 25% using the following operating conditions: experiments were conducted with mixtures of H_2, CO and nitrogen in a temperature range from 230 to 280°C, H_2/CO feed ratios of 1-1.5, pressure range of 4-16 bar

and GHSV=4500 h^{-1}. The catalytic test data are represented in Table 1. The stability of the catalyst was investigated by repetition of central points of the designs in the middle and the end of the experiments. The rate was kept constant at all points within the differential flow reactor reactor. The CO conversion and selectivity of olefin and paraffin products calculated according to Eqs. (1) and (2) respectively.

$$\text{CO conversion (\%)} = \frac{Moles\ of\ CO_{in} - Moles\ of\ CO_{out}}{Moles\ of\ CO_{in}} \times 100 \quad \ldots (1)$$

$$\text{Selectivity of } j \text{ product (\%)} = \frac{moles\ of\ carbon\ in\ product\ \text{j}}{moles\ of\ converted\ CO} \times 100 \quad \ldots (2)$$

The experimental reaction rate was determined as follows:

$$\text{Rate of CO conversion} = \frac{(\text{fractional conversion}) \times (\text{input flow rate of CO})}{\text{weight of the catalyst}} \quad \ldots (3)$$

Development of kinetic equations

In order to drive a proportion expression for CO consumption, the experiments were performed at pressures between 4 and 16 bar, temperatures between 230 and 280 °C and H_2/CO feed ratio between 1/1 and 1.5/1 to study the kinetic of FTS for hydrocarbons formation over the impregnated catalyst of 60%Co/40%Fe/90wt%SiO_2/1.5wt%K based on catalyst weight. The operating conditions and some results are shown in Table 1. The data obtained in these experiments are used in formulating rate expression for FTS reaction. The kinetic of FTS has been studied by researcher and many mechanistic schemes have been proposed, but among all the

Table 1 — Summary of experimental conditions and results for the kinetic tests at P_{Tot} = 4-16 bar, H_2/CO = 1-1.5 and GHSV= 4500 h^{-1}.

No. of data	T (°C)	P_{H_2} (bar)	P_{CO} (bar)	F_{CO} (mmol/min)	X_{CO} (%)	$-r_{CO} \times 10$ (mmol/gr cat. min)
1	230	1.534	1.547	2.774	3.161	0.877
2	240	1.557	1.555	2.734	2.749	0.752
3	250	1.585	1.563	2.695	7.436	2.00
4	270	1.37	1.485	2.466	16.92	4.18
5	230	3.088	3.087	5.535	3.470	1.92
6	240	3.075	3.082	5.418	3.699	2.00
7	230	4.928	4.979	8.927	2.338	2.09
8	241	4.802	4.632	8.127	3.493	2.84
9	260	6.028	5.997	10.147	6.295	6.39
10	270	5.862	5.945	9.874	10.149	10.02
11	250	0.983	1.023	1.764	19.882	3.51
12	260	0.944	0.992	1.678	22.388	3.76
13	273	0.84	0.976	1.612	23.569	3.80
14	280	0.845	0.975	1.590	23.895	3.80
15	277	1.634	1.928	3.161	24.565	7.77
16	280	2.83	2.869	4.679	24.254	11.81
17	283	3.213	3.721	6.036	24.00	14.48
18	240	1.967	1.216	2.138	5.078	1.09
19	250	1.915	1.195	2.061	6.686	1.38
20	258	1.663	1.099	1.867	14.092	2.63
21	240	3.819	2.388	4.198	6.763	2.84
22	250	3.757	2.366	4.080	7.573	3.09
23	260	3.34	2.205	3.731	13.872	5.18
24	240	5.713	3.601	6.330	6.2	3.92
25	250	5.457	3.506	6.046	8.702	5.26
26	260	4.887	3.248	5.496	15.423	8.48
27	270	4.829	3.274	5.438	18.351	9.98
28	230	7.836	4.858	8.710	5.081	4.43
29	240	7.553	4.779	8.401	6.659	5.59
30	250	7.378	4.707	8.117	8.025	6.51
31	270	6.383	4.303	7.147	15.949	11.39

proposed mechanisms in literature[19-25], the surface carbide and enolic mechanisms have been noted more than other mechanisms.

The carbide or carbene mechanism was proposed by Fischer and Tropsch in 1926[23]. In this mechanism, adsorbed CO is dissociated to C and O, the carbide is then hydrogenated to CH_x (the monomer). The methylene monomer polymerizes to surface alkyl species that terminate to products. It is widely supported despite the fact that it does not account for the formation of oxygenates. The hydoxycarbene or enol mechanism was proposed by Storch et al. in the 1950s[24]. In this mechanism, dissociative adsorption of H_2 and molecular adsorption of CO followed by the hydrogenation of adsorbed carbon monoxide by adsorbed hydrogen to form an oxygenated intermediate which reacts with another adsorbed hydrogen to form water and adsorbed carbon, and the reaction of the resulting carbon with adsorbed hydrogen as in the carbide mechanism. Although this mechanism explains the formation of oxygenates and was strongly supported by Kummer *et al.* who used C-alcohols or alkenes as a co-feed and observed that these alcohols participated in the chain growth[25], nevertheless, the details of the chemistry of this mechanism are unclear.

These two mechanistic cases were considered for the derivation of the model equations tested. In both cases, competitive adsorption on similar sites has been taken into account. For the determination of kinetic models, six mechanisms were offered on the basis of various monomer formation (elementary reactions) and carbon chain distribution pathways. An elementary reactions set on sites for each model is summarized in Table 2. In order to derive each kinetic model, initially one of the elementary reactions was assumed as a rate determination step and all other steps were considered at equilibrium. Then, all of the obtained models were fitted separately, against experimental data.

The development of the kinetic equations will be illustrated for model FT-III-3 (the third step elementary reaction from the FT-III model). The model codes refer to the set of elementary reactions and the elementary reaction is not at equilibrium (that is the rate-determining step, so in this case reaction 3). The reaction rate of the rate-determining step is:

$$-r_{\text{FT-III-3}} = k_3 \quad _{CO} \quad _{H} \qquad \ldots (4)$$

where $_{CO}$ is the surface fraction occupied with the associative adsorbed carbon monoxide and $_{H}$ is the surface fraction occupied with the dissociative adsorbed hydrogen. In this model it is assumed that only surface of CO occupy a significant fraction of the total number of sites. The fraction of vacant sites, θ_S, can be calculated from the following balance equation:

$$_{S} + \ _{CO} = 1 \qquad \ldots (5)$$

The surface fractions of CO and H can be calculated from the site balance, the preceding reaction steps which are at quasi-equilibrium:

Table 2 — Elementary reaction set for Fischer–Tropsch synthesis.

Model	No	Elementary reaction
FT-I	1	CO + S ↔ COs
	2	COs + s ↔ Cs + Os
	3	H_2 + 2s ↔ 2Hs
	4	Cs + Hs ↔ HCs + s
	5	HCs + Hs ↔ H_2Cs + s
	6	Os + Hs → HOs + s
	7	HOs + Hs → H_2Os + s
	8	H_2Os ↔ H_2O + s
FT-II	1	CO + s ↔ COs
	2	COs + s ↔ Cs + Os
	3	Cs + H_2 ↔ H_2Cs
	4	Os + H_2 → H_2Os
	5	H_2Os ↔ H_2O + s
FT- III	1	CO + s ↔ COs
	2	H_2 + 2s ↔ 2Hs
	3	COs + Hs ↔ HCOs + s
	4	HCOs+ Hs ↔ Cs + H_2Os
	5	Cs + Hs ↔ CHs + s
	6	CHs + Hs ↔ CH_2s +s
	7	H_2Os ↔ H_2O + s
FT- IV	1	CO + s ↔ Cos
	2	COs + s ↔ Cs + Os
	3	Cs + H_2 ↔ H_2Cs
	4	Os + H_2 → H_2O + s
	5	H_2 + 2s ↔ 2Hs
FT- V	1	CO + s ↔ Cos
	2	H_2 + 2s ↔ 2Hs
	3	Cos + Hs ↔ HCOs + s
	4	HCOs + Hs ↔ Cs + H_2O + s
	5	Cs + Hs ↔ CHs + s
	6	CHs + Hs ↔ CH_2s + s
	7	Os + Hs → HOs + s
	8	HOs + Hs → H_2O + 2s
FT-VI	1	CO + s ↔ COs
	2	COs + H_2 → CHs + OHs
	3	CHs + H_2 + s ↔ CH_2s + Hs
	4	OHs + Hs → H_2Os + s

$$CO + s \xleftrightarrow{k_1} COs$$
$$k_1 P_{CO\ S} - k_{-1\ CO} = 0 \quad \ldots (6)$$

$$_{CO} = K_1 P_{CO\ S}$$
$$K_1 = \frac{k_1}{k_{-1}} \quad \ldots (7)$$

where K_1 is the equilibrium constant of CO adsorption step.

$$H_2 + 2s \xleftrightarrow{k_2} 2Hs$$
$$k_2 P_{H_2\ S}^{\ 2} - k_{-2\ H}^{\ 2} = 0 \quad \ldots (8)$$

$$_{H} = K_2^{0.5} P_{H_2\ S}^{0.5}$$
$$K_2 = \frac{k_2}{k_{-2}} \quad \ldots (9)$$

where K_2 is the equilibrium constant of dissociated hydrogen adsorption step.

Substituting Eq. (7) into Eq. (5), the concentration of free active site can be expressed as:

$$_{S} = \frac{1}{1 + K_1 P_{CO}} \quad \ldots (10)$$

By substituting of the surface fraction of CO and H in Eq. (4), the final rate expression is obtained as follows:

$$-r_{\text{FT-III-3}} = \frac{k_3 K_1 K_2^{0.5} P_{CO} P_{H_2}^{0.5}}{(1 + K_1 P_{CO})^2} = \frac{k P_{CO} P_{H_2}^{0.5}}{(1 + a P_{CO})^2} \quad \ldots (11)$$

Table 3 summarizes the final form of the different rate expressions for the 7 possible kinetic models.

Results and Discussion

Catalyst screening results

The scanning electron microscopy (SEM) observations have shown differences in morphology of precursor and calcined catalysts (before and after the reaction at 8 bar and 260°C) The electron micrograph obtained from catalyst precursor depicts several agglomeration of particles and shows that this material comprise of particles with different size without any defined geometrical shapes; this material has a high density and homogeneous dispersion of particles (Fig. 1a). After the calcination at 550°C, the morphological feature was different to the precursor sample and showed that the agglomerate size was greatly reduced compared with the precursor (Fig. 1b). Therefore, the calcined catalyst before the test has disproportion agglomerate. However, the size of the tested grains grew larger by agglomeration (Fig. 1c), which may be due to sintering after the reactions. This is consistent with previous study by Galarrage *et al.*[26], who observed that temperature could cause agglomeration of these small grains, which correlates with catalyst deactivation under high temperature.

Table 3 — Reaction rate expression proposed for FTS

Model	Kinetic equation
FT-I-4	$-R_{CO} = \frac{k P_{H_2}^{0.5} P_{CO}^{0.5}}{(1 + a P_{CO}^{0.5} + b P_{H_2}^{0.5})^2}$
FT-I-5	$-R_{CO} = \frac{k P_{H_2}^{0.75} P_{CO}^{0.5}}{(1 + a P_{CO}^{0.5} P_{H_2}^{-0.25} + b P_{H_2}^{0.5})^2}$
FT-II-3	$-R_{CO} = \frac{k P_{H_2} P_{CO}^{0.5}}{(1 + a P_{CO}^{0.5} + b P_{CO})}$
FT-III-3	$-R_{CO} = \frac{k P_{CO} P_{H_2}^{0.5}}{(1 + a P_{CO})^2}$
FT-IV-3	$-R_{CO} = \frac{k P_{H_2} P_{CO}^{0.5}}{(1 + a P_{CO} + b P_{CO}^{0.5} + c P_{H_2}^{0.5})}$
FT-V-4	$-R_{CO} = \frac{k P_{H_2} P_{CO}}{(1 + a P_{CO} + b P_{H_2}^{0.5})^2}$
FT-VI-2	$-R_{CO} = \frac{k P_{CO}^{\ 0.5} P_{H_2}}{(1 + a P_{CO}^{0.5})}$

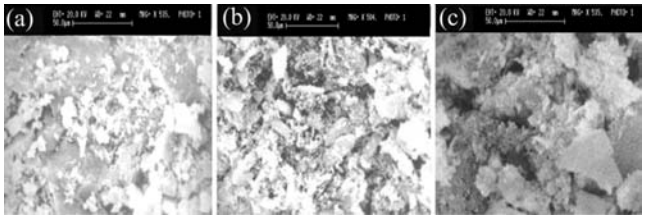

Fig. 1 — SEM images of 60%Co/40%Fe/90wt.%SiO_2/1.5wt.%K catalyst in (a) precursor; (b) catalyst before the test and (c) catalyst after the test (H_2/CO=1.25 at 8 bar and 260 °C).

The BET surface area measurement was used in order to measure the specific surface area of the catalysts. The specific surface area of the catalyst tested at the pressure of 8 bar and 260°C that is compared with the precursor and calcined catalysts before the test, is presented in Table 4. As shown, the calcined catalyst before the test has a higher specific surface area (105.8 m^2/g) than its precursor (97.2 m^2/g); this is in agreement with the SEM results which showed that the agglomerate size of calcined catalyst is less than its precursor and therefore leads to an increase in the BET specific surface area of the calcined sample. The high specific surface area of calcined catalyst before the test allows a high degree of metal dispersion[27].

Experimental results

It is generally accepted that operation condition variables such as temperature, pressure, H_2/CO feed ratio and gas space velocity influence the product distributions in FT synthesis. The catalyst was reduced in atmospheric pressure in a flow stream of H_2 with flow rate of 30 mL/min at 300°C for 12 h and then it was exposure the stream of H_2 + CO. 83 kinetic tests were carried out over 60%Co/40%Fe/90wt %SiO_2/1.5wt%K catalyst. The results at each particular condition are the calculated average value involving at least two measurements and the average value was considered as representative data.

Effect of temperature on products selectivity

The effect of reaction temperature on the catalytic performance of the 60%Co/40%Fe/90wt%SiO_2/1.5wt%K prepared using incipient impregnation procedure, was studied from the plots of product selectivity versus temperature and the results have shown at P = 8 bar, H_2/CO = 1.25 (Fig. 2) and P = 12 bar, H_2/CO = 1.25 (Fig. 3).

According to the obtained results (Figs 2 and 3), the optimum reaction temperature was 260 °C, at which temperature of the total selectivity of C_2–C_3 light olefin products was higher than those at the other reaction temperatures under the same operating conditions. The optimum temperature and pressure for different products are summarized in Table 5. The methane selectivity increased with increasing in temperature at constant pressure and H_2/CO = 1.25 feed ratio (Figs 2 and 3). The maximum selectivity with respect to ethylene and propylene occurs in 260°C and 280°C respectively as shown in Figs 2, 3 and Table 5.

Table 4 — BET surface area (m^2/g) results for both precursor and calcined catalysts (before and after reactor test at 8 bar and 260 °C)

Precursor	Calcined catalyst (before reaction)	Calcined catalyst (after reaction)
97.2	105.8	92.4

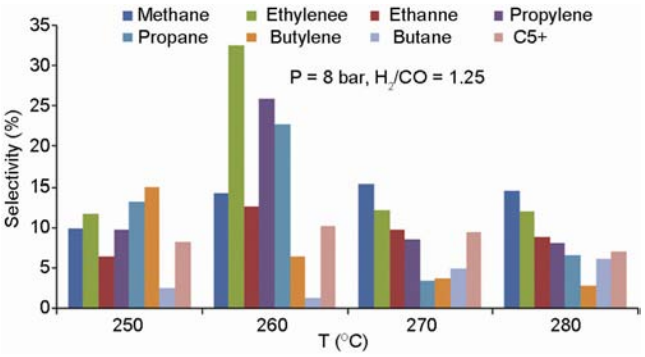

Fig. 2 — The effect of temperature on product selectivity at P = 8 bar and H_2/CO = 1.25

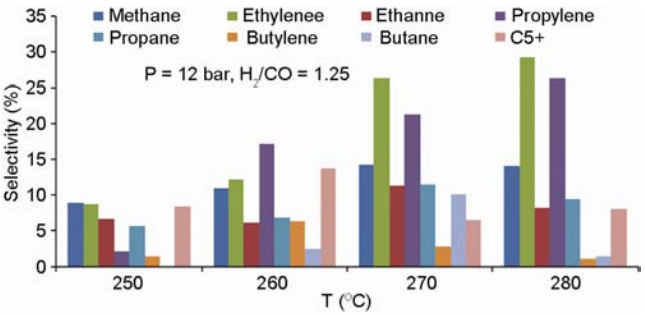

Fig. 3 — The effect of temperature on product selectivity at P = 12 bar and H_2/CO = 1.25

Effect of pressure on products selectivity

A series of experiments were carried out to investigate the influence of the reaction pressure on the catalytic performance of the cobalt iron oxide catalyst containing 60%Co/40%Fe/90wt%SiO_2/1.5wt%K for production of light olefins at GHSV = 4500 h^{-1}. The product selectivities at different temperatures of 260°C and 280°C and H_2/CO = 1.25 are plotted as a function of pressure (Figs 4 and 5). All these selectivity parameters reached steady-state values following a short initial period. With increasing total reaction pressure, methane and ethane selectivities remained unchanged or even slowly decreased, but the C_5^+ selectivity was increased. The results indicate that at the total pressure of 12 bar, the catalyst showed a total selectivity of 54% with respect to C_2–C_3 light olefins. However, the light olefins selectivities were changed and the results indicate that at the total pressure of 8 bar and 260°C, the catalyst showed

Table 5 — Optimum condition for product distribution in $H_2/CO = 1.25$.

Product	CH4	C_2H_4	C_2H_6	C_3H_6	C_3H_8	C_4H_8	C_4H_{10}	C_5^+
T (°C)	280	260	260	280	260	250	270	260
P (bar)	4	8	4	12	8	8	12	16
Selectivity (%)	16.6	32.55	14.95	26.17	22.77	15.0	10.12	14.06

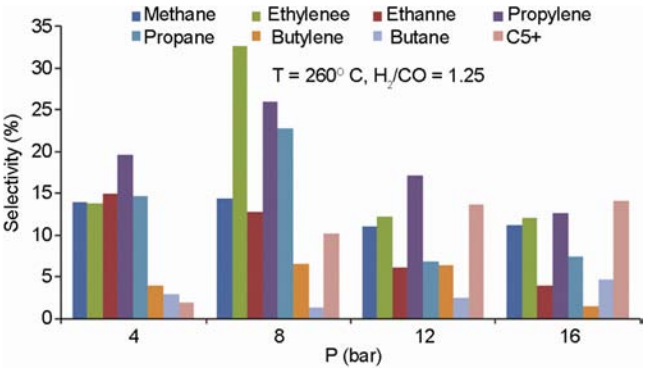

Fig. 4 — The effect of pressure on product selectivity at T = 260°C and $H_2/CO = 1.25$

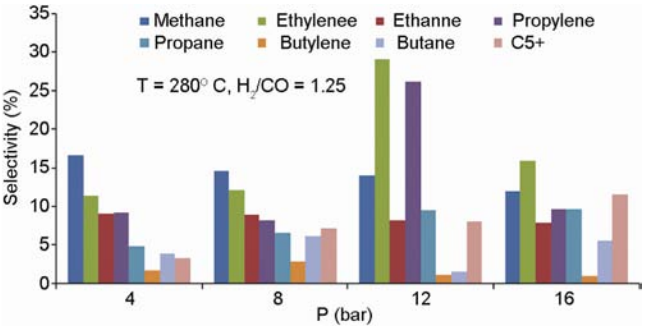

Fig. 5 — The effect of pressure on product selectivity at T = 280 °C and $H_2/CO = 1.25$

the highest total selectivity of 57% with respect to C_2–C_3 light olefins.

Kinetic study

The kinetic data presented in Table 1 for CO conversion were used for testing the seven models listed in Table 3. The discrimination of the kinetic models and the estimation of the kinetic parameters were performed by fitting the experimental data of the components partial pressure to the kinetics equations (Table 3). The estimation of the values of the kinetic parameters through best-fit model (FT-III-3) was better determined by a multi variable non-linear regression method, using the Levenberg-Marquardt algorithm. The objective function was to minimize the sum of the square of residuals corresponding to difference between the experimental data and those calculated for the kinetic models. The R^2 value (reflects the amount of variance), root mean square deviation (RMSD) and means absolute relative residual (MARR) have been reported as measure of the goodness of fit:

$$= \frac{1}{N_{\text{exp}}} \sum_{i=1}^{N_{\text{exp}}} r_{\text{CO,i}}^{\text{exp}} \qquad \ldots (12)$$

$$R^2 = 1 - \left(\frac{\sum_{i=1}^{N_{\text{exp}}} \left(r_{\text{CO, i}}^{\text{exp}} - r_{\text{CO, i}}^{\text{cal}} \right)^2}{\sum_{i=1}^{N_{\text{exp}}} \left(r_{\text{CO, i}}^{\text{exp}} - \quad \right)^2} \right)^2 \qquad \ldots (13)$$

and (RMSD) is described as:

$$\text{RMSD} = \frac{1}{N_{\text{exp}}} \left(\sum_{i=1}^{N_{\text{exp}}} \left(r_{\text{CO},i}^{\text{exp}} - r_{\text{CO},i}^{\text{cal}} \right)^2 \right)^2 \qquad \ldots (14)$$

The MARR between experimental and calculated consumption rate of CO is defined as:

$$MARR = \frac{1}{N_{\text{exp}}} \sum_{i=1}^{N_{\text{exp}}} \left(\frac{\left| r_{\text{i}}^{\text{exp}} - r_{\text{i}}^{\text{cal}} \right|}{r_{\text{i}}^{\text{exp}}} \right) \times 100 \qquad \ldots (15)$$

$r_{\text{CO,i}}^{\text{exp}}$ and $r_{\text{CO,i}}^{\text{cal}}$ indicate the experimental and calculated CO conversion rate from each kinetic model in *i*th data point, respectively, and N_{exp} clarify the number of experimental data points with pure error variance . To select the most suitable kinetic expression, different statistical indices can also be used to determine the quality of regression models. In order to find the most appropriate model, the following conditions should be considered[28]: obtained constants must be positive; coefficients of the equation must obey Arrhenius and Van't Hoff rules; optimal model is the one which gives the lowest MARR.

According to the statistical results obtained by inserting the data and models, the best model can be selected. Table 6 shows the statistical indicators for the FT kinetic models. Based on the statistical criteria

Table 6 — Estimated values of the statistical indicators for the FT kinetic models.

Model	Kinetic parameter					Statistical indicator		
	k_0 (x) (mmol g^{-1} min^{-1} bar^x)	a_0 (x) (bar^x)	b_0 (x) (bar^x)	c_0 (x) (bar^x)	E (kJ mol^{-1})	R^2	RMSD (10^{-5})	MARR (%)
FT-I-4	6.002E+02 (-1)	0.4958 (-1/2)	-0.0791 (-1/2)		92.41	0.929	1.67	18.28
FT-I-5	1.089E+04 (-5/4)	3.263 (-1/4)	2.060 (-1/2)		91.94	0.921	1.76	18.54
FT-II-3	1.352E+03 (-3/2)	1.103 (-1/2)	0.299 (-1)		91.79	0.924	1.73	18.37
FT-III-3	9.758E+03 (-3/2)	15.241 (-1)			106.02	0.942	1.49	16.43
FT-IV-3	7.78E+07 (-3/2)	-2.2E+05 (-1)	-1.3E+04 (-1/2)	2.E+04 (-1/2)	91.26	0.925	1.73	18.89
FT-V-4	9.12E+06 (-2)	2.08 (-1)	2.88 (-1/2)		91.89	0.933	1.62	17.87
FT-VI-2	2.49E+10 (-3/2)	5.33E+06 (-1/2)			107.32	0.849	2.66	22.82

and by comparing the values of R^2 and RMSD it was recognized that FT-III-3 is the most appropriate model. Also, it can be seen that FT-III-3 model has the lowest MARR among the other models that has been used in the present study. This value is reasonable and shows that the predicted values are 16.43% different from the observed values. Therefore, there are best fitted by a LHHW approach rate form $-r_{CO} = k P_{CO} P_{H_2}^{0.5}/(1+a P_{CO})^2$ which the controlling step of the reaction rate is formation of monomer CHO intermediate. Model FT-III-3 shows that dominant mechanism on catalyst surface is based on dissociation of hydrogen with associative carbon monoxide and forming methyl monomers (enolic mechanism), which is same as the previous study done by the Wojciechowski[29]. In previous research on bimetallic cobalt catalysts (titania-supported Co–Mn catalyst)[1], forming of the monomer CH_2 was done by reaction of adsorbed CO and hydrogen in two steps that was assumed as dominant mechanism. Also Keyser *et al.*[30] observed through a study on bimetallic Co-Mn oxide catalyst that a reaction rate equation for the FT reaction based on the enolic mechanism gave results which were marginally better than results based on the carbide mechanism. As it has been shown in Table 6, the activation energy for the best fitted model (FT-III-3) was found to be 106.2 kJ mol^{-1} which is close to activation energies reported previously: 100 and 103 kJ mol^{-1} reported by Yang *et al.*[31] and Storch *et al.*[24], respectively. Nevertheless, it was substantially lower than the value of 142 kJ mol^{-1} reported by Reuel and Bartholomew[32]. However, Reuel and Bartholomew's value was obtained at significantly lower reactant partial pressure and was based on only two data points, while in this study it was based on thirty one data points. The activation energy obtained for hydrocarbon formation suggests that the diffusion interference is not significant in the experiments[33]. As with intraparticle diffusion limitations, the presence of external mass-transfer limitations could be detected via measuring the apparent activation energy. An external mass-transfer control regime could lead to the apparent energy activation of just a few kJ mol^{-1} (Ref 34).

Conclusion

The silica-supported cobalt-iron catalyst with potassium-promoted was prepared by impregnation method and was tested for hydrogenation of carbon monoxide to light olefins. The kinetic experimental study was performed in a differential micro-fixed-bed-reactor by altering reaction pressure (4-16 bar), H_2/CO feed molar ratio (1-1.5) and space velocity (4500 h^{-1}) at the temperature range of 230-280°C. Considering Langmuir-Hinshelwood-Hogan-Watson adsorption theory in catalytic reactions, CO consumption rate equations were defined by 6 mechanisms, consequently, 7 kinetic models were proposed. Intrinsic kinetic data obtained in the initial rate region show that the enolic mechanism with interaction between adsorption CO and dissociated adsorption hydrogen as the rate controlling step gives the most plausible kinetic model. The kinetic parameters estimated for this kinetic model presented reasonable confidence intervals. The product distributions in FT synthesis are strongly influenced by temperature and pressure, and 260°C and 8 bar are the optimum temperature and pressure for obtaining C_2-C_3 light olefins hydrocarbons with high selectivity. The activation energy for the best fitted model was 106.2 kJ mol^{-1}; this value of activation energy confirms that intraparticle mass transport is not significant.

References

1 Atashi H, Siami F, Mirzaei A A & Sarkari M, *J Ind Eng Chem*, 16 (2010) 952.

2 Mansouri M, Atashi H, Mirzaei A A & Jangi R, *Int J Ind Chem*, 4 (2013) 1.

3 Mirzaei A A, Beig babaei A, Galavy M & Youssefi A, *Fuel Process Technol*, 91 (2010) 335.

4 Cabet C, Roger A C, Kiennemann A, LÃkamp S & Pourroy G, *J Catal*, 173 (1998) 64.

5 Tihay F, Roger A C, Kiennemann A & Pourroy G, *Catal Today*, 58 (2000) 263.

6 de la Peña O'Shea V A, Alvarez-Galvan M C, Campos-Martin J M & Fierro J L G, *Appl Catal A*, 326 (2007) 65.

7 de la Peña O'Shea V A, Alvarez-Galvan M C, Campos-Martin J M, Mene´ndez N N, Tornero J S D & Fierro J L G, *Eur J Inorg Chem*, 2006 (2006) 5057.

8 Nakhaei Pour A, Shahri S M K, Bozorgzadeh H R, Zamani Y, Tavasoli A & Marvast M A, *Appl Catal A*, 348 (2008) 201.

9 Zennaro R, Tagliabue M & Bartholomew C H, *Catal Today*, 58 (2000) 309.

10 Mirzaei A A, Shirzadi B, Atashi H & Mansouri M, *J Ind Eng Chem*, 18 (2012) 1515.

11 Mansouri M, Atashi H & Setareshenas N, *Detailed Kinetic Study of the FTS over the co-precipitated Co-Ce/SiO_2* (Lambert Academic Publishing, Saarbrüchen- Germany), 2013.

12 Atashi H, Mansouri M, Hosseini S H, Khorram M, Mirzaei A A, Karimi M & Mansouri G, *Korean J Chem Eng*, 29 (2012) 304.

13 Mansouri M, Atashi H, Farshchi Tabrizi F, Mansouri G & Setareshenas N, *Int J Ind Chem*, 5 (2014) 1.

14 van der Laan G P & Beenackers A A C M, *Catal Rev -Sci Eng*, 41 (1999) 255.

15 Huff Jr G A & Satterfield C N, *Ind Eng Chem Process Des Dev*, 23 (1984) 696.

16 Yates I C & Satterfield C N, *Energy & Fuels*, 5 (1991) 168.

17 van Steen E & Schulz H, *App Catal A*, 186 (1999) 309.

18 Outi A, Rautavuoma I & van der Baan H S, *Appl Catal*, 1 (1981) 247.

19 Mansouri M, Atashi H, Farshchi Tabrizi F, Mirzaei A A & Mansouri G, *J Ind Eng Chem*, 19 (2013) 1177.

20 Visconti C G, Tronconi E, Lietti L, Zennaro R & Forzatti P, *Chem Eng Sci*, 62 (2007) 38.

21 Botao T, Jie C, Haijun W, Jiqing L, Shaocheng Z, Ya L, Ying L & Xiaohui G, *Chin J Catal*, 28 (2008) 687.

22 Yang J, Liu Y, Chang J, Wang Y, Bai L, Xu L, Xiang H, Li Y & Zhong B, *Ind Eng Chem Res*, 42 (2003) 5066.

23 Fischer F & Tropsch H, *Brennst Chem*, 7 (1926) 97.

24 Storch H H, Golumbic N & Anderson R B, *The Fischer-Tropsch Synthesis and Related Synthesis* (Wiley, New York), 1951.

25 Kummer J T, Podgurski H H, Spencer W B & Emmett P H, *J Am Chem Soc*, 73 (1951) 564.

26 Galarrage C E, *Heterogeneous catalyst for the synthesis of middle distillate hydrocarbons*, M.Sc. Thesis, University of Western Qntario, London, 1998.

27 Bechara R, Balloy D, Dauphin J -Y & Grimblot J, *Chem Mater*, 11 (1999) 1703.

28 Bercic G & Levec J, *Ind Eng Chem Res*, 31 (1992) 1035.

29 Wojciechowski B W, *Catal Rev - Sci Eng*, 30 (1988) 629.

30 Keyser M J, Everson R C & Espinoza R L, *Ind Eng Chem Res*, 39 (2000) 48.

31 Yang C H, Massoth F E & Oblad A G, *Adv Chem Ser*, 178 (1979) 35.

32 Reuel R C & Bartholomew C H, *J Catal*, 85 (1984) 78.

33 Sari A, Zamani Y & Taheri S A, *Fuel Process Technol*, 90 (2009) 1305.

34 Khodakov A Y, Chu W & Fongarland P, *Chem Rev*, 107 (2007) 1692.